Visual Snapshots of Intracellular Kinase Activity at the Onset of Mitosis

Zhaohua Dai,[1,2] Natalya G. Dulyaninova,[1] Sanjai Kumar,[1] Anne R. Bresnick,[1,*] and David S. Lawrence[1,3,*]
[1]Department of Biochemistry, The Albert Einstein College of Medicine of Yeshiva University, 1300 Morris Park Avenue, Bronx, NY 10461, USA
[2]Forensic Science Program and the Department of Chemistry and Physical Sciences, Pace University, 1 Pace Plaza, New York, NY 10038, USA
[3]Present address: The Departments of Chemistry, Medicinal Chemistry and Natural Products, and Pharmacology, Campus Box 3290, Kenan Laboratories, The University of North Carolina at Chapel Hill, Chapel Hill, NC 27599, USA.
*Correspondence: bresnick@aecom.yu.edu (A.R.B.), lawrencd@email.unc.edu (D.S.L.)

SUMMARY

Visual snapshots of intracellular kinase activity can be acquired with exquisite temporal control by using a light-activatable (caged) sensor, thereby providing a means to interrogate enzymatic activity at any point during the cell-division cycle. Robust protein kinase activity transpires just prior to, but not immediately after, nuclear envelope breakdown (NEB). Furthermore, kinase activity is required for the progression from prophase into metaphase. Finally, the application of selective protein kinase C (PKC) inhibitors, in combination with the caged sensor, correlates the action of the PKC β isoform with subsequent NEB.

INTRODUCTION

Cellular biochemistry is commonly assessed by using lysates or cell-free model systems. However, in order to directly correlate enzymatic activity with cellular behavior, new tools must be developed to visualize the action of enzymes in cells, tissues, and, ultimately, living organisms. Fluorescent microscopy provides the instrumental means by which to observe intracellular biochemistry, but this methodology is dependent on the design and construction of fluorescent sensors that can report changes in the catalytic status of the target enzyme. However, live-cell microscopy places unique demands on the sensor. In particular, sensors that possess short-wavelength fluorophores or exhibit modest enzyme-induced fluorescent changes are insufficient for visualizing enzyme-catalyzed reactions in living cells. The small volume of a typical mammalian cell requires the fluorophore to be both bright and highly responsive to its enzymatic target. Furthermore, the fluorophore must possess the proper photophysical properties (i.e., long-wavelength excitation and emission) so that the endogenous fluorophores present in the cell do not interfere with the readout. Finally, the multitude of biochemical transformations transpiring in

the cell at any given time requires that the sensor be reasonably selective for its enzymatic target.

In addition to the concerns noted above, live-cell enzymology offers a unique challenge that, in general, has no counterpart in experiments that utilize pure enzymes or cell lysates. One of the attractive features associated with observing enzyme action in the natural intracellular environment is that catalytic activity can be correlated with cellular behavior. However, although the investigator controls the start and stop points of enzyme-catalyzed reactions in a typical cuvette-based experiment, the biochemical apparatus of the cell controls the timing and duration of intracellular enzymatic activity. The loss of investigator control in live-cell enzymology has important ramifications. For example, if the intracellular enzyme of interest is constitutively active, then the time required for loading the sensor into the cell could preclude the acquisition of well-defined kinetics. In addition, since intracellular enzymatic activity can cycle on and off, the absence of a fluorescent response in live-cell assays may not necessarily be due to the absence of enzymatic activity, but it could be a consequence of sensor consumption at an earlier stage. Finally, loading any unnatural molecular entity into a cell, particularly via microinjection or various cell-permeablizing delivery systems, can stress the cell and thus generate an artificial response. As a consequence, it is common practice to allow the cell to recover after the introduction of proteins, peptides, nucleic acids, etc. For these reasons, as well as others, it would prove advantageous to devise reagents (inhibitors, sensors, substrates, etc.) that can be delivered to the cell in an inert form, but ones that are sensitive to subsequent activation upon demand. In this regard, light-activatable species offer the possibility of precise temporal control over sensor activity even after the reagent has entered the cell [1].

Protein kinase activity is critical for the G2/M transition [2–6], particularly at or around the time of nuclear envelope breakdown (NEB). However, it is unknown if activity is present prior to, during, or after NEB in living cells. We recently described the PKC sensor 1 (Figure 1), an efficient substrate for the conventional protein kinase C (PKC) isoforms (α, β, and γ) [7]. This peptide exhibits a readily observable fluorescent change upon phosphorylation. However, using sensor 1, we found that PKC is constitutively
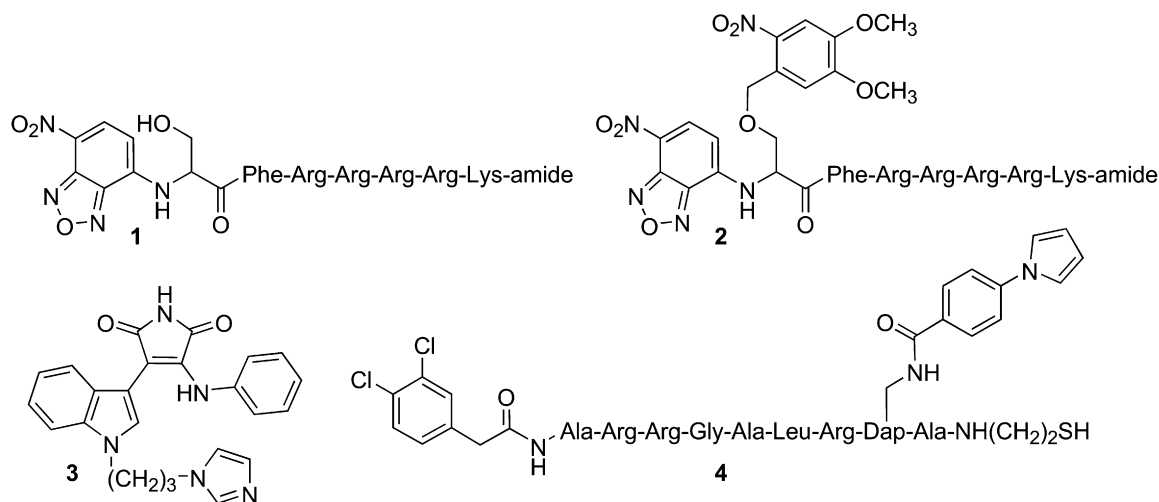
Figure 1. Structures of PKC Sensors and Inhibitors

Compound **1** responds to PKC-catalyzed phosphorylation in a fluorescently sensitive fashion [7]. The nonphosphorylatable analog, **2**, is converted to the active sensor, **1**, by photolysis [8]. Compound **3** is a selective PKC β inhibitor [11], whereas compound **4** serves as a selective PKC α inhibitor [12].

active in interphase cells unless these cells have been serum starved [7]. Consequently, the issue of sensor consumption (i.e., complete phosphorylation of peptide **1**) prior to the key biological event (e.g., NEB) represents a significant concern. By contrast, the corresponding caged version, **2** (Figure 1), is not susceptible to phosphorylation until it is photolyzed, which then furnishes the active sensor, **1** [8]. In short, the caged derivative, **2**, can be loaded into cells and subsequently used to visualize kinase activity at any time point relative to NEB, without having to resort to artificial constraints (e.g., serum starvation). We have employed compound **2** to assess intracellular protein kinase activity at precise time intervals just prior to, during, and immediately after NEB. In addition, in combination with known protein kinase inhibitors, we have identified the kinase responsible for both the phosphorylation of the active sensor, **1**, as well as mitotic progression from prophase to metaphase.

RESULTS AND DISCUSSION

Peptide 1 as a Substrate for the PKC Isoforms Present in PtK2 Cells

The PtK2 cell line was employed in this study because these cells remain flat during mitosis and have large chromosomes that allow for ready identification of the individual stages of mitosis. Western blot analysis revealed that PtK2 cells express the α, β, ι, μ, θ, and ζ isoforms (Figure 2). We've previously shown that **1** is an outstanding substrate for PKC α, β, and γ [7]. The first two isoforms are present in PtK2 cells, whereas PKC γ is not (Figure 2). In addition, we've found that peptide **1** serves as a weak substrate for ι, θ, and ζ isoforms. Finally, the fluorescent sensor is not phosphorylated by PKC μ (Figure 3). These results appear to be consistent with the previously described substrate specificity of some of these isoforms [9]. The conventional isoforms, α and β, are known to prefer sub-

strates that possess positively charged residues (in particular Arg) at the +2 and +3 positions relative to the phosphorylatable Ser moiety (i.e., -Ser-Xaa-Arg-Arg). However, members of the novel and atypical PKC subfamilies generally prefer hydrophobic residues at +2 and +3, although they can tolerate positively charged amino acids at these positions as well. In addition to the PKC family of enzymes, a variety of other protein kinases have been implicated as participants in the onset of mitosis [10]. However, these enzymes either fail to (Akt-1, AurB, Cdc-2, Plk1) or only weakly (Nek2) phosphorylate peptide **1**.

An Assessment of Protein Kinase Activity at the Prophase-to-Metaphase Transition

The caged peptide, **2** (200 μM in needle; 2–20 μM final intracellular concentration), and 70 kDa Texas red-dextran (5 μM in needle) were coinjected into PtK2 cells. The Texas red-dextran is excluded from the intact nucleus and thus provides an easily visualized readout of NEB, which transpires over a period of ∼2 min (Figure 4A; Movies S1 and S2, see the Supplemental Data available with this article online). In general, photolysis (1 s) of individual cells during prophase generates a time-dependent increase in fluorescence (Figure 4A), followed by NEB. Interestingly, the few cells (3 out of 18) that failed to display a fluorescence change in prophase also failed to undergo subsequent NEB, suggesting that the former is required for the latter to transpire. As a control, we found that microinjection with buffer alone results in a fraction of cells that do not progress to NEB (8 out of 30). Apparently, the stress of microinjection can have deleterious consequences in a small fraction of cells in terms of mitotic progression. Nevertheless, the majority of cells (>80%) microinjected with sensor share several key enzymological and behavioral properties: (a) a fluorescent enhancement observed until NEB in all cells that exhibit subsequent NEB, (b) a rate of fluorescence change that levels off as the nuclear envelope

Figure 2. Western Blots of PKC Isoforms Present in Ptk2 Cells

collapses, and (c) generally unchanged fluorescence after NEB. These results are consistent with the notion that PKC is active prior to NEB but is rendered inactive after nuclear collapse. However, another interpretation is that all sensor molecules have been phosphorylated by the time the cell reaches the NEB signpost. Consequently, the experiments outlined in Figure 4A were repeated, but the caged peptide, **2**, was photoactivated immediately after NEB, as signified by the appearance of Texas red-dextran within the former nuclear region. Under these conditions, there was no significant change in reporter fluorescence intensity (14 out of 16 cells exhibited no fluorescence change, and 2 out of 16 cells displayed a <15% fluorescence change) for up to 9 min after NEB (Figure 4B). These results suggest that kinase activity is biochemically switched off after the collapse of the nuclear envelope. Finally, we also established that the post-NEB phosphorylation state of peptide **1** is not altered by intracellular phosphatases because we failed to observe any change in fluorescence (8 of 10 cells displayed no fluorescence change, and 2 out of 10 exhibited a <15% fluorescence change) in the presence of the general phosphatase inhibitor okadaic acid (Figure 4C).

Protein Kinase Inhibitors Establish PKC β as the Sensor Kinase

Although the sensor experiments expose a clean demarcation in kinase activity prior to and immediately after
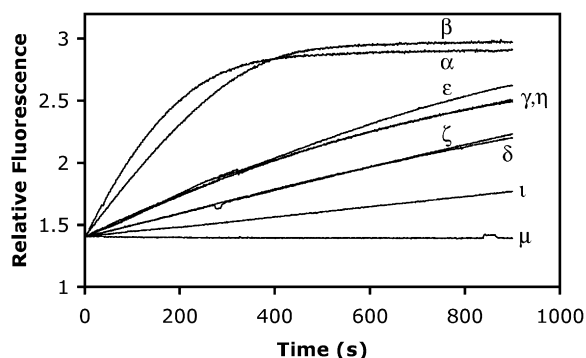
NEB, they do not reveal which kinase is responsible for sensor phosphorylation, nor do they establish a kinase-dependent cause and effect with nuclear collapse. As noted above, Nek2 as well as the α, β, ι, μ, θ, and ζ isoforms of PKC are capable of catalyzing the phosphorylation of peptide **1**. Inhibitors that selectively target each of these individual enzymes would be helpful in assessing which of these kinases is responsible for sensor phosphorylation. In addition, these inhibitors could prove particularly useful in correlating the activity of a specific kinase with the subsequent NEB signpost.

Compound **3** (Figure 1) has been reported to be a selective PKC β inhibitor compared to the α and ε isoforms [11]. However, its selectivity compared to other PKC isoforms has not been explicitly addressed. Consequently, in addition to PKC α and β, we examined the inhibitory potency of this derivative against the other isoforms present in PtK2 cells, namely, ι, μ, θ, and ζ. Compound **3** exhibits an IC_{50} of 11 ± 1 nM for the βII isoform, which is consistent with the previously reported value of 5 nM [11]. By contrast, the IC_{50} values for the other PKC isoforms are significantly larger. The IC_{50} for PKC α is 1.3 ± 0.1 μM, and there is no observable inhibition for the ι, μ, θ, or ζ isoforms or the Nek2 protein kinase when **3** is present at 50 μM. Consequently, compound **3** serves as a highly selective inhibitor for the β isoform. With this in mind, we examined the effect of compound **3** (12 μM in the cell media) on mitotic progression. We found that 65% of PtK2 cells (20 out of 31 cells) did not proceed from prophase into metaphase in the presence of **3**. These results indicate that passage through NEB is not dependent upon Nek2, nor on the ι, μ, θ, or ζ PKC isoforms, because compound **3** does not inhibit these enzymes at 12 μM. However, the 12 μM concentration of the indolylmaleimide, **3**, required to establish an NEB block in the majority of the cells is ~10-fold greater than the IC_{50} value for PKC α and is significantly greater than that for PKC β obtained under in vitro conditions. Consequently, although use of compound **3** rules out Nek2 and the ι, μ, θ, or ζ PKC isoforms as effectors of peptide **1** phosphorylation and NEB, it does not allow us to conclusively distinguish between the PKC α or β isoforms as the sensor **1** kinases.

The PKC α inhibitor, **4** (Figure 1, K_i = 800 pM), displays a 385-fold selectivity compared to PKC β and an even greater selectivity compared to the other PKC isoforms
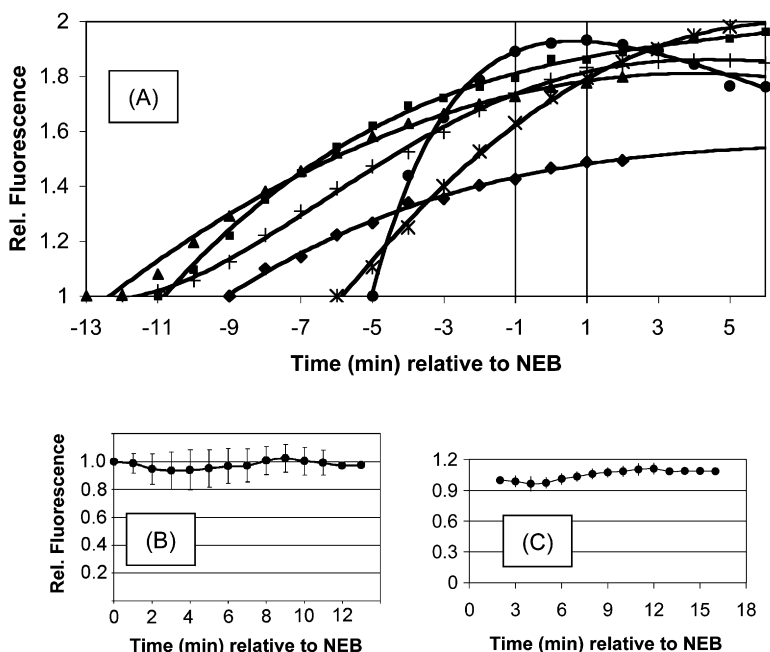

Figure 3. PKC Isoform-Catalyzed Phosphorylation of Peptide 1 as a Function of Time

Figure 4. Protein Kinase Activity prior to and after Nuclear Envelope Breakdown

(A) Time course of the phosphorylation of peptide **1** prior to NEB. The nonphosphorylatable analog, **2**, and 70 kD Texas red-dextran were simultaneously microinjected into PtK2 cells. Cells were illuminated (1 s) during prophase (i.e., prior to NEB) to convert the inert sensor, **2**, to its active form, **1**, and the fluorescence change as a function of time was recorded with respect to NEB. Each progress curve is derived from a single cell, and a total of 18 cells were examined (6 of the progress curves are shown here).

(B) Time course of the phosphorylation of peptide **1** after NEB. PtK2 cells were treated as in Figure 2A, except that photolysis was performed after NEB. The progress curve represents the average fluorescence change of 16 cells (each data point represents the mean ± SD).

(C) Fluorescence change after NEB in the presence of okadaic acid (1.5 μM).

[12]. The caged sensor, **2**, and Texas red-dextran were co-injected along with two different concentrations of the PKC α-selective inhibitor, **4**: 2 mM (intracellular concentration: 20–200 μM) and 1 μM (intracellular concentration: 10–100 nM). The cells were photolyzed to convert the caged sensor, **2**, into the active species, **1**. Under the first set of conditions (i.e., 2 mM inhibitor **4**), both PKC α and β should be inhibited, whereas under the latter conditions (i.e., 1 μM inhibitor **4**), only the activity of PKC α should be compromised. Cells microinjected with 2 mM inhibitor **4** fail to exhibit PKC activity and do not progress through NEB (n = 10 cells). By contrast, cells injected with a 1 μM stock solution of the PKC α-selective inhibitor, **4**, exhibit both PKC activity and NEB (12 out of 15 cells). In short, compound **3** blocks sensor **1** phosphorylation as well as NEB at a concentration that is only consistent with catalysis by either PKC α or β. Subsequent studies with compound **4** eliminated PKC α as the kinase sensor, thereby suggesting that PKC β is the intracellular peptide **1** kinase required for NEB. The results are consistent with those reported by Fields and coworkers, who first identified PKC β as a mitotic lamin kinase [4–6].

Ptk2 cells express both the type I and type II isoforms of PKC β. These otherwise identical enzymes differ only in their C-terminal 50/52 amino acids [13]. Unfortunately, there are no reported inhibitors or substrates that discriminate between these two closely related enzymes. There have been several reports describing the differential translocation of βI and βII in response to environmental stimuli [14–16]. For example, Becker and Hannun have shown that both isoforms, when overexpressed in HeLa cells, are diffusely distributed throughout the cytoplasm and excluded from the nucleus [16]. Upon phorbol ester stimulation, however, βI migrates exclusively to the plasma membrane, whereas βII is positioned at both the plasma

membrane as well as a juxtanuclear location. To the best of our knowledge, the distribution of the two PKC β isoforms has not been examined as a function of cell cycle. Immunocytochemistry revealed a marked difference in the localization of βI and βII in nonmitotic cells. βI is predominantly associated with the nucleus, both during interphase and in prophase (Figure 5). Furthermore, since the isoform is excluded from the nucleolus, this implies that βI is present in the nucleus itself and is not merely associated with the nuclear membrane (the latter would generate a uniform distribution about the nucleus). By contrast, βII is distributed throughout the cytoplasm during interphase (Figure 5). Upon entry into prophase, the subcellular distribution of βI remains unchanged, namely, this isoform
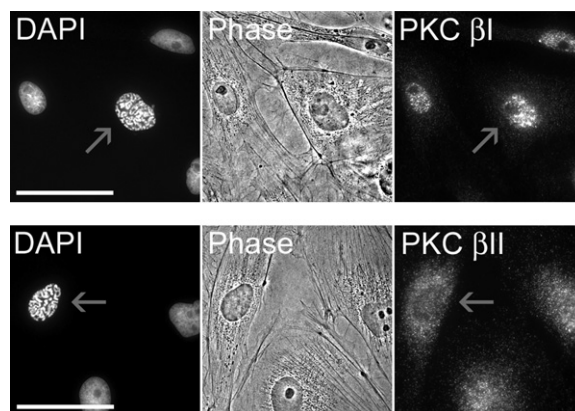

Figure 5. Localization of PKC β Isoforms in Prophase
Cells stained with PKC βI (upper panel) or PKC βII (lower panel) antibodies and DAPI. The arrows highlight cells in prophase. All other cells are in interphase. The scale bar is 50 μm.

retains its association with the nucleus. By contrast, βII undergoes a partial subcellular redistribution as it accumulates at or near the nuclear boundary. In short, the subcellular distribution of both isoforms is consistent with a role in promoting nuclear collapse (i.e., via lamin phosphorylation). However, it is tempting to speculate that the cycle-dependent accumulation of βII at the periphery of the nucleus may be significant, particularly with respect to subsequent NEB.

Previous studies primarily employed cell-free systems to implicate PKC β as a lamin kinase activated prior to NEB [4]. In addition, these studies employed cell lysates, which were obtained from a large population of chemically induced synchronized cells. Unfortunately, cells released from aphidicolin or nocodazole blockades rarely progress through the division cycle as a uniform population. Furthermore, some cell lines, such as PtK2 cells, cannot be synchronized. The latter is especially unfortunate given the utility of this particular cell line as the exemplary model system by which to study mitosis. Perhaps most importantly, however, lysates from large cell populations are simply not ideal for examining short, yet critical time points, which encompass key cellular events. By contrast, the light-activatable sensor, **2**, provides a temporally precise method by which to interrogate protein kinase activity in an investigator-controlled fashion. In particular, we found that protein kinase activity is vigorous just prior to NEB, but is abruptly switched off after NEB. Furthermore, in combination with selective protein kinase inhibitors, we identified PKC β as the protein kinase that phosphorylates sensor **1** prior to nuclear envelope collapse.

SIGNIFICANCE

Live-cell enzymology represents unique challenges that generally do not need to be confronted in studies with pure enzymes or cell lysates. In particular, the cell, and not the investigator, controls the timing of enzymatic activity. Caged analogs of sensors, inhibitors, substrates, and other biologically active species offer a means by which to retain control over reagent activity even after it has entered the cell. In short, light-activatable species allow the investigator to choose, with high temporal precision, when to assess, alter, or otherwise control intracellular enzymology. We employed this strategy to evaluate protein kinase C (PKC) activity in the minutes immediately prior to, during, and after nuclear envelope breakdown (NEB), the mitotic landmark that serves as the transition from prophase to metaphase. Activation of the sensor in an investigator-controlled temporally precise fashion revealed that intracellular protein kinase activity is vigorous just prior to NEB, but is abruptly switched off after nuclear collapse. An array of PKC isoform-selective inhibitors was employed to demonstrate that PKC β serves as the mitotic kinase that catalyzes the phosphorylation of the sensor and drives the transition from prophase to metaphase.

EXPERIMENTAL PROCEDURES

Spectrofluorometric Assays

All spectrofluorometric measurements were carried out on a Photon Technology QM-1 Instrument at 30°C. The photomultiplier tube setting was held constant at 1000 V during all measurements. The assay volume and pH were maintained at 200 μl and 7.5, respectively. The reaction was initiated by the addition of enzyme (10 μl) into the sensor (compound **1**) assay buffer solution (190 μl), and the time-dependent change in fluorescence intensity (λ_{ex} = 520 nm; λ_{em} = 560 nm) was continuously monitored. For a direct comparison of relative activities of various PKC isoforms and other protein kinases toward sensor **1**, all measurements were carried out under optimum experimental conditions for the enzymes. For (A) PKC α, β, and γ: 62.5 mM HEPES (pH 7.5), MgCl$_2$ (3 mM), CaCl$_2$ (0.3 mM), EGTA (0.1 mM), ATP (1 mM), DTT (1 mM), PS (0.1 mg/ml), DAG (0.1 mg/ml), enzyme (50 nM), and compound **1** (100 μM); (B) PKC ζ and ι: 62.5 mM HEPES (pH 7.5), MgCl$_2$ (10 mM), EGTA (0.5 mM), PS (0.04 mg/ml), ATP (1 mM), DTT (1 mM), enzyme (50 nM), and compound **1** (100 μM); (C) PKC μ, ε, δ, θ, and η: 62.5 mM HEPES (pH 7.5), MgCl$_2$ (10 mM), EGTA (0.5 mM), PS (0.04 mg/ml), DAG (0.01 mg/ml), ATP (1 mM), DTT (1 mM), enzyme (50 nM), and compound **1** (100 μM); (D) Nek2: 50 mM Tris-HCl buffer (pH 7.5), MgCl$_2$ (10 mM), DTT (1 mM), ATP (1 mM), enzyme (50 nM), and compound **1** (100 μM); (E) Cdc2: 50 mM Tris-HCl buffer (pH 7.5), MgCl$_2$ (10 mM), DTT (2 mM), EGTA (1 mM), Brij 35 (0.01%), enzyme ("2 units"), and compound **1** (100 μM); (F) Akt: 20 mM Tris-HCl buffer (pH 7.5), MgCl$_2$ (10 mM), DTT (5 mM), enzyme (50 nM), and compound **1** (100 μM); (G) Plk1: 50 mM HEPES buffer (pH 7.5), MgCl$_2$ (10 mM), DTT (2.5 mM), Triton X-100 (0.01%), enzyme (50 nM), and compound **1** (100 μM); (H) Aurora kinase B: 50 mM Tris-HCl buffer (pH 7.5), MgCl$_2$ (10 mM), enzyme (50 nM), and compound **1** (100 μM).

IC$_{50}$ Determination of PKC β Inhibitor 3 against PKC Isoforms

All inhibition studies were performed by using the [γ-^{33}P]ATP radioactive method in a 96-well plate format at 30°C. Optimal conditions (including specific peptide substrates) were chosen for the classical, novel, and atypical PKC isoforms as follows: (A) PKC α and βII: an assay volume of 50 μl/well was used. Thus, the assay involving 100 μM ATP was performed as follows. A 20 μl aliquot of inhibitor **3**, appropriately diluted in 1:4 DMSO:H$_2$O, was added (final concentration = 3310, 1655, 827.5, 413.75, 206.87, 103.4, 51.7, 25.6, 12.9, and 0 nM) to 20 μl assay buffer to give a final concentration of 62.5 mM HEPES (pH 7.5), MgCl$_2$ (10 mM), EGTA (0.5 mM), CaCl$_2$ (0.8 mM), DAG (17.6 μg/ml), PS (100 μg/ml), peptide substrate Ac-Ser-Phe-Arg-Arg-Arg-Arg-NH$_2$ (75 μM), and cold ATP (100 μM or 1 mM), supplemented with 1.5 μCi/well [γ-^{33}P]ATP for radioactive detection. The reaction was initiated with the addition of 10 μl enzyme buffer containing 20 mM Tris (pH 7.5), PKC (final concentration = 0.1 ng/μl), BSA (final concentration = 0.15 mg/ml), EDTA (final concentration = 0.2 mM), and DTT (final concentration = 0.2 mM). The reaction was allowed to progress for 15 min at 30°C and was quenched subsequently with 6% phosphoric acid (100 μl). An aliquot of 75 μl quenched reaction mixture was transferred to P81 cellulose phosphate paper unifilter plates, and the solution was allowed to stand for 12 min. The solution was then filtered off, and the membrane was washed with 0.1% phosphoric acid (4×), followed by water. The scintillation fluids (100 μl) were then added, and counting was performed on a 1420 MicroBeta counter (Perkin Elmer). The rate of reaction was assessed by the incorporation of ^{33}P into the peptide substrate. (B) PKC μ: performed as described above, except that CaCl$_2$ was not added and the peptide substrate Ala-Ala-Leu-Val-Arg-Gln-Met-Ser-Val-Ala-Phe-Phe-Phe-Lys-OH (EMD Biosciences) was employed at a final concentration of 60 μM. (C) PKC ι and ζ: performed as described above, except that CaCl$_2$ and DAG were not added and the peptide substrate Ac-Pro-Arg-Lys-Arg-Gln-Gly-Ser-Val-Arg-Arg-Arg-Val-NH$_2$ was employed at a final concentration of 75 μM. SigmaPlot, Enzyme Kinetics 1.1, was used for data analyses.

Western Blots

Cells were lysed (Laemmli sample buffer containing chymostatin, leupeptin, and pepstatin), and proteins were separated on a 4%–20% Tris-HCl SDS-PAGE gel and subsequently transferred overnight onto a Immuno-Blot PVDF membrane at 4°C. The membrane was incubated with 5% nonfat dry milk solution in Tris Buffer Saline with Tween (0.05%) for 1 hr, and the membrane was incubated with primary antibodies in 5% nonfat dry milk solution in TBS-T for 3 hr at room temperature. The following dilutions of primary antibodies were used, as recommended by the manufacturers: PKC α (1:500); β1 (1:500); βII (1:500); θ (1:200); μ (1:1000); ζ (1:1000); ι (1:200); γ (1:1000); δ (1:500); ε (1:1000); η (1:1000); λ (1:1000). After incubation with primary antibody, the membrane was washed with TBS-T for 15 min (2×) and treated for 1 hr at room temperature with secondary antibodies (1:2000 dilution) conjugated to horseradish peroxidase (HRP). The membrane was subsequently washed for 15 min (2×) with TBS-T and treated with HRP substrate (Pierce Supersignal West Pico Chemiluminescent Substrate) for 1 min, and the chemiluminescent signal was detected on film.

Live-Cell Enzymology

PtK2 cells were cultured at 37°C for 2–3 days (70%–80% confluence) on 50 mm MatTek glass-bottom dishes (MatTek Corp, Ashland, MA) containing photo-etched gridded coverslips (thickness 0.19–0.22 mm) in Dulbeco's MEM with nonessential amino acids and 10% FBS in a humidified atmosphere containing 5% CO_2. Prior to microinjection, the dishes were washed three times with PBS, and then 4 ml L-15 medium (without phenol red) supplemented with 10% FBS was added. The caged sensor, **2** (synthesized and characterized as previously described [8]), was dissolved in PBS at a concentration of 200 μM and prefiltered through a 0.22 μm centrifuge filter. Cells were microinjected with the 200 μM caged sensor and 1 μM 70K dextran tagged with Texas red (Molecular Probes, Eugene, OR) by using a commercial microinjection system (Transjectors 5246, Eppendorf, Westbury, NY) at an estimated final concentration of 2–20 μM for the caged peptide and 10–100 nM Texas red-dextran. The estimate for dilution via microinjection was obtained from the equation for volume (V) flow through a capillary tube ($V/t = \pi p r^4/8 l \eta$), where p is the difference in pressure at the ends of the tube (290 hPa), r is the radius (0.05 μm), l is the length (10 μm) of the tube, η is the viscosity of the injected solution (0.69 × 10^{-2} g/cm −s), and t is the total injection time (0.3 s). The average volume of a fibroblast is taken as 2 pl [17]. Cells were exposed to UV illumination from a 100 W Hg-Arc lamp (by using a set of 2 KG5 heat filters in the light path and a narrow band pass DAPI filter of 355 ± 10 nm) through a PlanApo 40× N.A. 0.75 objective for 1 s to activate the sensor (i.e., only cells in the immediate microscopic field were illuminated). Immediately after UV treatment, time-lapse images were collected with 2 × 2 binning by using a Cooke Sensicam QE cooled CCD camera (driven by IPlab software) mounted on an Olympus 1X70 inverted microscope (Melville, NY) with a PlanApo 40×, 0.75 N.A. objective in conjunction with a 1.5× "booster" slider, and a FITC filter set with an excitation wavelength of 460–500 nm and an emission wavelength of 510–560 nm. A long working distance condenser (N.A. 0.55) was used. Images were collected every minute for 9–30 min (1000 ms exposure time). The digitized images were analyzed by using ImageJ to measure the mean intensity of the whole cell. Images and fluorescence intensity measurements were also obtained from control cells that were injected with the same caged sensor in the presence of 200 μM staorosporine to make photobleaching adjustments. For experiments involving the PKCβ inhibitor, **3**, or the phosphatase inhibitor okadaic acid, cells were incubated with the relevant inhibitor for at least 1 hr prior to microinjection.

Immunofluorescence

To examine the distribution of PKC βI and II isoforms throughout the cell cycle, PtK2 cells growing on glass coverslips were fixed in freshly prepared 3.7% formaldehyde in PBS for 15 min, permeabilized for 20 s with −20°C acetone, immediately rehydrated in PBS containing 0.02% azide, and blocked in PBS containing 1% bovine serum albumin (BSA).

Cells were then incubated with primary PKC βI (C-16) sc-209 or PKC βII (C-18) sc-210 rabbit polyclonal antibodies (Santa Cruz Biotechnology) at a dilution of 1:100 in PBS containing 1% BSA for 1 hr at room temperature. After washing with 1% BSA in PBS, cells were incubated with a Cy3-conjugated donkey anti-rabbit antibody (Jackson ImmunoResearch Lab) at a dilution of 1:500 in 1% BSA in PBS for 40 min at room temperature and rinsed again. Coverslips were incubated with DAPI (Sigma) at 0.1 μg/ml in 1% BSA in PBS for 10 min before mounting in Pro-Long Antifade (Molecular Probes). Immunofluorescence images were acquired by using IPLab Spectrum software (Scanalytics, Inc.) and a CoolSNAP HQ interline 12-bit, cooled CCD camera (Roper Scientific) mounted on an Olympus IX70 microscope with a PlanApo 60×, 1.4 N.A. objective (Olympus) and HiQ bandpass filters (Chroma Technology Corp.). Images were processed by using Photoshop (Adobe Systems).

Supplemental Data

Supplemental Data include two movies and are available online at http://www.chembiol.com/cgi/content/full/14/11/1254/DC1/.

REFERENCES

1. Lawrence, D.S. (2005). The preparation and in vivo applications of caged peptides and proteins. Curr. Opin. Chem. Biol. 9, 570–575.

2. Black, J.D. (2000). Protein kinase C-mediated regulation of the cell cycle. Front. Biosci. 5, 406–423.

3. Murray, N.R., Burns, D.J., and Fields, A.P. (1994). Presence of a βII protein kinase C-selective nuclear membrane activation factor in human leukemia cells. J. Biol. Chem. 269, 21385–21390.

4. Hocevar, B.A., Burns, D.J., and Fields, A.P. (1993). Identification of protein kinase C (PKC) phosphorylation sites on human lamin B. J. Biol. Chem. 268, 7545–7552.

5. Goss, V.L., Hocevar, B.A., Thompson, L.J., Stratton, C.A., Burns, D.J., and Fields, A.P. (1994). Identification of nuclear β II protein kinase C as a mitotic lamin kinase. J. Biol. Chem. 269, 19074–19080.

6. Thompson, L.J., and Fields, A.P. (1996). βII protein kinase C is required for the G2/M phase transition of cell cycle. J. Biol. Chem. 271, 15045–15053.

7. Yeh, R.-H., Yan, X., Cammer, M., Bresnick, A.R., and Lawrence, D.S. (2002). Real time visualization of protein kinase activity in living cells. J. Biol. Chem. 277, 11527–11532.

8. Veldhuyzen, W.F., Nguyen, Q., McMaster, G., and Lawrence, D.S. (2003). A light-activated probe of intracellular protein kinase activity. J. Am. Chem. Soc. 125, 13358–13359.

9. Nishikawa, K., Toker, A., Johannes, F.J., Songyang, Z., and Cantley, L.C. (1997). Determination of the specific substrate sequence motifs of protein kinase C isozymes. J. Biol. Chem. 272, 952–960.

10. Ferrari, S. (2006). Protein kinase controlling the onset of mitosis. Cell. Mol. Life Sci. 63, 781–795.

11. Tanaka, M., Sagawa, S., Hoshi, J., Shimoma, F., Matsuda, I., Sakoda, K., Sasase, T., Shindo, M., and Inaba, T. (2004). Synthesis of anilino-monoindolylmaleimides as potent and selective PKCß inhibitors. Bioorg. Med. Chem. Lett. 14, 5171–5174.

12. Lee, J.H., Nandy, S.K., and Lawrence, D.S. (2004). A highly potent and selective PKCα inhibitor generated via combinatorial modification of a peptide scaffold. J. Am. Chem. Soc. *126*, 3394–3395.

13. Ono, Y., Kikkawa, U., Ogita, K., Fujii, T., Kurokawa, T., Asaoka, Y., Sekiguchi, K., Ase, K., Igarashi, K., and Nishizuka, Y. (1987). Expression and properties of two types of protein kinase C: alternative splicing from a single gene. Science *236*, 1116–1120.

14. Becker, K.P., and Hannun, Y.A. (2004). Isoenzyme-specific translocation of protein kinase C (PKC) βII and not PKCβI to a juxtanuclear subset of recycling endosomes: involvement of phospholipase D. J. Biol. Chem. *279*, 28251–28256.

15. Goodnight, J.A., Mischak, H., Kolch, W., and Mushinski, J.F. (1995). Immunocytochemical localization of eight protein kinase C isozymes overexpressed in NIH 3T3 fibroblasts. Isoform-specific association with microfilaments, Golgi, endoplasmic reticulum, and nuclear and cell membranes. J. Biol. Chem. *270*, 9991–10001.

16. Disatnik, M.H., Winnier, A.R., Mochly-Rosen, D., and Arteaga, C.L. (1994). Distinct responses of protein kinase C isozymes to c-erbB-2 activation in SKBR-3 human breast carcinoma cells. Cell Growth Differ. *5*, 873–880.

17. Kislauskis, E.H., Zhu, X.-C., and Singer, R. (1997). β-actin messenger RNA localization and protein synthesis augment cell motility. J. Cell Biol. *136*, 1263–1270.